

“WEATHER” VARIABILITY OF CLOSE-IN EXTRASOLAR GIANT PLANETS

KRISTEN MENO^{1,2,3}, JAMES Y-K. CHO,^{4,5} SARA SEAGER,⁵ AND BRADLEY M. S. HANSEN⁶

Received 2002 August 30; accepted 2003 February 28; published 2003 March 20

ABSTRACT

Shallow-water numerical simulations show that the atmospheric circulation of the close-in extrasolar giant planet (EGP) HD 209458b is characterized by moving circumpolar vortices and few bands/jets (in contrast to ~ 10 bands/jets and the absence of polar vortices on cloud-top Jupiter and Saturn). The large spatial scales of moving circulation structures on HD 209458b may generate detectable variability of the planet’s atmospheric signatures. In this Letter, we generalize these results to other close-in EGPs, by noting that shallow-water dynamics is essentially specified by the values of the Rossby (Ro) and Burger (Bu) dimensionless numbers. The range of likely values of Ro ($\sim 10^{-2}$ to 10) and Bu (~ 1 –200) for the atmospheric flow of known close-in EGPs indicates that their circulation should be qualitatively similar to that of HD 209458b. This results mostly from the slow rotation of these tidally synchronized planets.

Subject headings: planetary systems — planets and satellites: general — stars: atmospheres — turbulence

1. INTRODUCTION

The focus of extrasolar planet research has broadened to now include the characterization of their physical properties, as shown by the recent sodium detection in the atmosphere of HD 209458b (Charbonneau et al. 2002). Atmospheric circulation is expected to play a key role in determining a number of observational characteristics of extrasolar giant planets (EGPs), including their albedo and transmission spectrum (see, e.g., Seager & Sasselov 1998, 2000; Sudarsky, Burrows, & Pinto 2000; Brown 2001). This is especially true for close-in EGPs, which are thought to be tidally locked to their parent star and irradiated on one side only: circulation will be essential in redistributing heat from the day to the night side on these planets, thus determining to a large extent how they will appear to the distant observer (Cho et al. 2003; J. Y-K. Cho, K. Menou, B. M. S. Hansen, & S. Seager 2003, in preparation; Showman & Guillot 2002).

Recently, we have presented a set of detailed shallow-water numerical simulations of the atmospheric flow on HD 209458b (Cho et al. 2003; J. Y-K. Cho et al. 2003, in preparation), currently the only EGP with known mass and radius from the transit light curves and radial velocity measurements (Charbonneau et al. 2000; Henry et al. 2000; Mazeh et al. 2000; Jha et al. 2000; Brown et al. 2001). These simulations suggest that, contrary to the simple day/night (hot/cold) picture, the circulation on this planet is characterized by two moving circumpolar vortices and a small number of latitudinal bands/jets. The vortices act as dynamically distinct thermal spots whose motion around the poles generates variability as seen by an observer interested in quantities integrated over the planetary disk (or circumference).

It is possible to determine the general features of the cir-

ulation pattern expected within the framework of shallow-water dynamics by specifying the two dimensionless numbers—Rossby (Ro) and Burger (Bu)—for the atmospheric flow. In this Letter, we estimate a range of likely Ro and Bu values for known close-in EGPs and conclude that their atmospheric circulation pattern should be qualitatively similar to that of HD 209458b. In § 2, we recall how the atmospheric flow pattern can be characterized by the knowledge of Ro and Bu. In § 3, we describe the sample of close-in EGPs selected for our study and how we estimate likely values for various global planetary parameters entering into the definition of Ro and Bu. Finally, our results and conclusions are presented in § 4.

2. TURBULENT SHALLOW-WATER DYNAMICS

Shallow-water equations describe the motion of a thin, homogeneous layer of hydrostatically balanced, inviscid fluid with a free surface, in motion around a rotating planet (Pedlosky 1987; Holton 1992). The fluid is subject to gravitational and Coriolis forces and obeys the following equations:

$$\frac{\partial \mathbf{v}}{\partial t} + \mathbf{v} \cdot \nabla \mathbf{v} = -g \nabla h - f \mathbf{k} \times \mathbf{v}, \quad (1)$$

$$\frac{\partial h}{\partial t} + \mathbf{v} \cdot \nabla h = -h \nabla \cdot \mathbf{v}, \quad (2)$$

where \mathbf{v} is the horizontal velocity, h is the thickness of the modeled layer, $f = 2\Omega \sin \varphi$ is the Coriolis parameter, Ω is the rotation rate of the planet, φ is the latitude, g is the gravitational acceleration, and \mathbf{k} is the unit vector normal to the surface of the planet. In dimensionless form, shallow-water equations become functions only of the Rossby (Ro) and Burger (Bu) numbers:

$$\text{Ro} \equiv \frac{U}{|f|L}, \quad (3)$$

$$\text{Bu} \equiv \left(\frac{L_D}{L}\right)^2, \quad L_D \equiv \sqrt{gH}/|f|, \quad (4)$$

where U , L , and H are characteristic velocity, length, and layer thickness scales, respectively; L_D is the Rossby deformation

¹ Chandra Fellow.

² Current address: Department of Astronomy, University of Virginia, P.O. Box 3818, Charlottesville, VA 22903.

³ Department of Astrophysical Sciences, Princeton University, Peyton Hall, Princeton, NJ 08544.

⁴ Spectral Sciences, Inc., 99 South Bedford Street, No. 7, Burlington, MA 01803.

⁵ Department of Terrestrial Magnetism, Carnegie Institution of Washington, 5241 Broad Branch Road, NW, Washington, DC 20015.

⁶ Division of Astronomy, University of California at Los Angeles, 8971 Math Sciences, Los Angeles, CA 90095.

radius. Note that $|f| \sim \Omega$ at midlatitudes and that the planetary radius, R_p , is the relevant length scale when discussing the large-scale atmospheric circulation. The Rossby number measures the importance of rotation on the flow, while the Burger number measures the stratification of the atmosphere via the Brunt-Väisälä frequency (Holton 1992).

The atmospheric structure in bands of gaseous giant planets in our solar system is well described as emerging from freely evolving shallow-water turbulence on the sphere (Cho & Polvani 1996b). Turbulence in a thin atmospheric layer is quasi-two-dimensional in nature. Contrary to the forward turbulent energy cascade observed in three-dimensional geometry, two-dimensional turbulence is characterized by an inverse energy cascade (transfer from small to large scales) and a forward cascade of enstrophy⁷ down to small scales, where it is dissipated by viscous processes. Qualitatively, the inverse cascade is associated with the growth of vortices through continuous mergers.

Turbulence in a thin atmospheric layer is also strongly constrained by the combined effect of spherical geometry and rotation (the “ β -effect”). While the force balance is everywhere the same along a latitude circle, it changes with latitude because of the dependence of the Coriolis term with φ . This anisotropy, as measured by the parameter $\beta = 2\Omega \cos \varphi / R_p$ (the latitudinal gradient of f), is strongest at the equator, where β is maximum. While fluid motions are free to grow to the largest available scale in the longitudinal direction, their growth is limited in the latitudinal direction by the characteristic Rhines scale, $L_\beta = \pi(2U/\beta)^{1/2}$ (Rhines 1975). This anisotropic growth is a likely origin of the banded structure on gaseous giant planets in our solar system; the number of bands expected for a given planet is roughly $N_{\text{band}} \sim \pi R_p / L_\beta$.

Cho & Polvani (1996a) presented an extensive numerical study of freely evolving shallow-water turbulence. They explored the entire parameter space of the equations, as determined by the two dimensionless numbers Ro and Bu. They showed that the anisotropy due to the β -effect on a rotating sphere is necessary but not sufficient to produce a long-lasting banded structure. The Rossby deformation radius, L_D , must also be $\lesssim R_p/3$ for the banded structure to be stable. This small value of L_D , which acts as a limiting scale for vortex interactions, prevents the formation (via successive mergers) of large-scale structures such as circumpolar vortices.

J. Y-K. Cho et al. (2003, in preparation) present a generalization of the results of Cho & Polvani in the case when the planet is subject to dayside hemispheric heating, as expected for close-in EGPs. Dayside heating was prescribed in the adiabatic limit by forcing the fluid to be permanently thicker on that side, while keeping the average thickness constant. Extensive exploration of the parameter space of the forced model showed that previous shallow-water dynamics results were recovered even in the presence of this extraforcing (i.e., L_β and L_D remain the relevant scales determining the number of bands and the formation of polar vortices).

These results can be recast in terms of the values of Ro and Bu for the atmospheric flow. By setting $L \sim R_p$, $|f| \sim \Omega$, and $\beta \sim \Omega/R_p$ (midlatitudes), we see that the number of bands/jets expected is $N_{\text{band}} \sim 1/(2\text{Ro})^{1/2}$ and that the presence of circumpolar vortices is expected for $\text{Bu} \gtrsim \frac{1}{2}$. Thus, if the values of Ro and Bu for other close-in EGPs can be estimated, one can get an idea of the type of large-scale atmospheric circulation

⁷ The flow enstrophy is defined as $\frac{1}{2}\xi^2$, where $\xi = \mathbf{k} \cdot \nabla \times \mathbf{v}$ is the flow vorticity.

expected on these planets in the stable, radiative region. In our estimates of Ro and Bu, we will set $U = \bar{U}$, which is the global velocity scale of the atmospheric flow and is only known for the solar system giants (Table 1).

An important parameter entering the definition of both Ro and Bu is the planetary rotation rate, Ω . While the value of Ω is generally unknown for EGPs, a number of close-in EGPs have the advantage of being probably tidally synchronized to their parent star, so that their rotation rate has effectively been measured via the orbital period ($\Omega = \Omega_{\text{orb}}$ for circular orbits). As we show below, the knowledge of Ω for this sample of close-in EGPs restricts the range of possible values for Ro and Bu to a small enough region of the parameter space that their atmospheric circulation pattern can be inferred.

3. SAMPLE OF CLOSE-IN EXTRASOLAR GIANT PLANETS

Since tidal synchronization occurs faster than orbital circularization, it is possible that some close-in EGPs with substantial eccentricities are nonetheless (pseudo)synchronized (i.e., synchronized at the periastron orbital frequency). The shallow-water results described in § 2 were established only in the limit of negligible eccentricity, however. Hence, we must restrict our sample to planets with small eccentricities.⁸ Table 1 lists all the EGPs selected for our study, plus the four solar system giants. Parameters for the EGPs were collected from the extrasolar planet almanac⁹ and encyclopedia.¹⁰

Low-eccentricity EGPs were divided into two groups, based on their orbital distance to the parent star. In the first group, EGPs with semimajor axes $a \leq 0.066$ AU are most likely tidally synchronized since all known EGPs with such small values of a are also circularized. The tidal synchronization status of the more distant planets (in the second group) is less clear because several eccentric EGPs with distances of closest approach¹¹ as small as 0.05 AU are also known. It is thus not clear why some EGPs with periastron distances larger than this value would be tidally circularized while others would not. We note, however, that for values of the tidal parameter Q not too different from that of Jupiter ($\sim 10^5$), EGPs in this second group are also expected to be synchronized. We will assume it is indeed the case in our calculations.

Radial velocity surveys only measure $M_p \sin i$, which is a lower limit to the planet’s mass, M_p , given the unknown orbital inclination, i . For randomly oriented systems, the distribution of $\cos i$ is uniform. We adopt the value of M_p corresponding to $\sin i = 0.5$ for our fiducial estimate of Ro and Bu, and we allow $\sin i$ to vary from 0.1 to 1 when estimating the range of likely values for Ro and Bu.¹²

For a given mass, M_p , the radius of an isolated planet is estimated from the mass-radius relation for substellar objects of Chabrier & Baraffe (2000), supplemented at the low-mass end by a constant density law that empirically fits values for the solar system giants. To account for the slower cooling under strong stellar irradiation, we also allow the radius to be up to

⁸ We limit the eccentricity of planets in our sample to $e \lesssim 0.1$, by analogy with the small eccentricities of solar system giants to which “zero-eccentricity” shallow-water models have been applied with success (Cho & Polvani 1996b; J. Y-K. Cho et al. 2003, in preparation).

⁹ See <http://exoplanets.org/almanacframe.html>.

¹⁰ See <http://www.obspm.fr/encycl/encycl.html>.

¹¹ The periastron distance, where tidal forces are the strongest, is also roughly the circular radius expected for the orbit after complete circularization.

¹² Note that for low values of $\sin i$, some EGPs in Table 1 have $M_p > 13 M_{\text{Jup}}$ and are thus brown dwarfs. We expect shallow-water results to be applicable even in that limit.

TABLE 1
GLOBAL PLANETARY PARAMETERS

Planet (1)	M_* (M_\odot) (2)	P_{orb} (days) (3)	a (AU) (4)	e (5)	M_p (M_{Jup}) (6)	R_p (m) (7)	g (m s^{-2}) (8)	Ω (s^{-1}) (9)	H (m) (10)	\bar{U} (m s^{-1}) (11)	Ro (12)	Bu (13)
Neptune	1.0	60189.0	30.05	0.0113	0.054	2.5×10^7	11	9.75×10^{-5}	3×10^4	300	1.2×10^{-1}	5.6×10^{-2}
Uranus	1.0	30685.4	19.20	0.0457	0.046	2.6×10^7	9	$(-1) \times 10^{-4}$	3.5×10^4	300	1.2×10^{-1}	4.8×10^{-2}
Saturn	1.0	10759.2	9.58	0.0565	0.30	6.0×10^7	9	1.6×10^{-4}	4×10^4	300	3.2×10^{-2}	3.9×10^{-3}
Jupiter	1.0	4332.6	5.20	0.0489	1.00	7.1×10^7	23	1.8×10^{-4}	2×10^4	50	4.0×10^{-3}	2.8×10^{-3}
Group 2												
Rho CrB b	0.95	39.6450	0.2300	0.0280	>1.100	1.8×10^{-6}	0.24–7.4	68–180
HD 195019b	1.02	18.3000	0.1400	0.0500	>3.430	4.0×10^{-6}	0.10–4	30.8–69.6
Gl 86b	0.79	15.7800	0.1100	0.0460	>4.000	4.6×10^{-6}	0.09–3.4	13.2–46.4
55 Cnc b	0.95	14.6530	0.1150	0.0200	>0.840	5.0×10^{-6}	0.084–2.8	13.2–39.2
HD 130322b	0.79	10.7240	0.0880	0.0480	>1.080	6.8×10^{-6}	0.062–2	6.8–18
Group 1												
HD 168746b	0.92	6.4090	0.0660	0.0000	>0.240	1.1×10^{-5}	0.036–1.92	3.2–22.4
HD 49674b	1.00	4.9400	0.0600	0.0000	>0.120	1.5×10^{-5}	0.030–1.88	2.4–23.6
Ups And b	1.30	4.6170	0.0590	0.0340	>0.710	1.6×10^{-5}	0.026–0.96	2.44–8.0
51 Peg b	0.95	4.2300	0.0512	0.0130	>0.440	1.6×10^{-5}	0.024–1.04	1.64–7.6
HD 209458b	1.05	3.5247	0.0450	0.0000	0.690	10^8	8	2.1×10^{-5}	2×10^6	...	0.024–0.48	3.6
HD 75289b	1.05	3.5100	0.0460	0.0540	>0.420	2.1×10^{-5}	0.024–0.88	1.32–6.0
BD –10316b	1.10	3.4870	0.0460	0.0000	>0.480	2.1×10^{-5}	0.020–0.84	1.36–6.0
Tau Boo b	1.30	3.3120	0.0500	0.0000	>4.090	2.2×10^{-5}	0.019–0.72	1.36–4.96
HD 179949b	1.24	3.0930	0.0450	0.0500	>0.840	2.4×10^{-5}	0.018–0.62	1.20–3.56
HD 187123b	1.06	3.0900	0.0420	0.0300	>0.520	2.4×10^{-5}	0.019–0.72	1.08–4.4
HD 46375b	1.00	3.0240	0.0410	0.0000	>0.249	2.4×10^{-5}	0.017–0.90	1.0–6.4
HD 83443b	0.79	2.9853	0.0380	0.0800	>0.350	2.4×10^{-5}	0.017–0.80	0.80–6.4

NOTE.—Col. (1): In order of decreasing orbital period. Col. (2): Stellar mass. Col. (3): Orbital period. Col. (4): Semimajor axis. Col. (5): Eccentricity. Col. (6): Planet mass. Col. (7): Planet radius. Col. (8): Surface gravity. Col. (9): Rotation rate. Col. (10): Atmospheric scale height. Col. (11): Global atmospheric velocity scale. Col. (12): Rossby number. Col. (13): Burger number.

50% larger than the value for an isolated planet, in agreement with published cooling EGP models (Burrows et al. 2000; Guillot & Showman 2002). Our results depend only weakly on the planetary radius, as long as $R_p \sim R_{\text{Jup}}$ (as expected for all masses of interest). The gravitational acceleration is derived as $g = GM_p/R_p^2$, where G is the gravitational constant.

For the mean layer thickness, H , we adopt the atmospheric pressure scale height, $H_{\text{atm}} \equiv \mathcal{R}T_{\text{atm}}/g$, where \mathcal{R} is the perfect gas constant. The global radiative equilibrium temperature of the planet is $T_{\text{atm}} = T_*(R_*/2a)^{1/2}(1 - A_B)^{1/4}$, which is a function of the parent star luminosity ($L_* \propto T_*^4 R_*^2$), the planet's semimajor axis a , and Bond albedo A_B . We adopt $A_B = 0.5$ for all our numerical estimates; our results only weakly depend on the value of A_B unless it approaches unity. The stellar luminosity is derived from the mass through the simple mass-luminosity relation $L_* = (M_*/M_\odot)^{3.6} L_\odot$.

The last two parameters needed to determine Ro and Bu are the planetary rotation rate Ω and the global kinetic energy scale \bar{U} . We assume that $\Omega = \Omega_{\text{orb}}$ (as determined by radial velocity surveys) in all cases. We allow \bar{U} to vary from 50 m s^{-1} , the smallest observed value for giant planets in the solar system (Jupiter), to 1000 m s^{-1} , a rather large value for which the typical wind speeds in the atmosphere of hot, close-in EGPs approach the sound speed. A value $\bar{U} = 400 \text{ m s}^{-1}$ is adopted for our fiducial estimate of Ro and Bu.

4. RESULTS

Estimated values for Ro and Bu are given in Table 1 for solar system giants and close-in EGPs. The values listed for close-in EGPs correspond to the range of minimum/maximum values found given the various assumptions detailed in § 3. Fiducial estimates are also reported in Figure 1, where filled circles correspond to group 1 EGPs (safe tidal synchronization

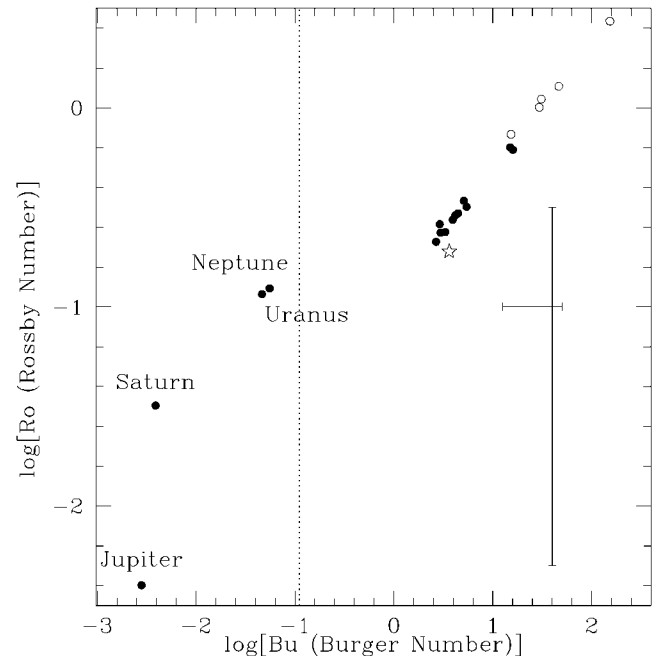


FIG. 1.—Location of solar system and close-in EGPs in the Rossby-Burger space. The assumption of tidal synchronization for extrasolar planets represented by filled circles is the safest (group 1; see Table 1). HD 209458b is indicated by a star symbol. A representative range of possible values around the fiducial estimates for extrasolar giant planets (each individual filled or open circle) is shown as an error bar (see Table 1 for details). Formation of circumpolar vortices is expected in the region to the right of the vertical dotted line ($\text{Bu} \gtrsim \frac{1}{2}$). A larger number of bands are expected for smaller values of Ro (see text for details).

assumption) and open circles to group 2 EGPs (tidal synchronization assumption less safe). HD 209458b is indicated by a star symbol.

It is clear from Figure 1 that close-in EGPs, as a group, occupy a different region of the Ro-Bu parameter space than solar system giants. In particular, they systematically have a Burger number $Bu > \frac{1}{9}$ (even when accounting for the large range of allowed values; Table 1), which indicates that the presence of circumpolar vortices is expected in the radiative region of close-in EGPs, within the framework of shallow-water dynamics. The larger values of Ro also indicate that generally few bands/jets are expected on these planets (the uncertainty on \bar{U} strongly affects this number; see Table 1), thus allowing the formation of larger “great spots” (which could also contribute to the variability; J. Y-K. Cho et al. 2003, in preparation). The near alignment of all the points representing close-in EGPs in Figure 1 shows that the dominant parameter determining their position in this diagram is their rotation rate ($Ro \propto \Omega^{-1}$; $Bu \propto \Omega^{-2}$). The small values of Ro and Bu for solar system giants reflect their relatively fast rotation rates.

Although we argued in favor of variable atmospheric signatures for close-in EGPs, it is important to note that models do not yet quantitatively predict how much variability is expected. In Cho et al. (2003) and J. Y-K. Cho et al. (2003, in preparation), we emphasize that the combination of \bar{U} (unknown) and the amplitude of day-night heating (parametrized in adiabatic simulations) determines the contrast of the thermal spots associated with circumpolar vortices. In the future, diabatic shallow-water models will allow a self-consistent determination of the day-night forcing. More sophisticated models, combined with detailed radiative transfer and chemistry descriptions (Seager & Sasselov 1998, 2000; Seager, Whitney, & Sasselov 2000), will allow us to make quantitative predictions regarding the level of variability expected for various atmospheric signatures.

Support for this work was provided by NASA through Chandra Fellowship grant PF9-10006 awarded by the Smithsonian Astrophysical Observatory for NASA under contract NAS8-39073.

REFERENCES

- Brown, T. M. 2001, *ApJ*, 553, 1006
 Brown, T. M., Charbonneau, D., Gilliland, R. L., Noyes, R. W., & Burrows, A. 2001, *ApJ*, 552, 699
 Burrows, A., et al. 2000, *ApJ*, 534, L97
 Chabrier, G., & Baraffe, I. 2000, *ARA&A*, 38, 337
 Charbonneau, D., Brown, T. M., Latham, D. W., & Mayor, M. 2000, *ApJ*, 529, L45
 Charbonneau, D., Brown, T. M., Noyes, R. W., & Gilliland, R. L. 2002, *ApJ*, 568, 377
 Cho, J. Y-K., Menou, K., Hansen, B. M. S., & Seager, S. 2003, *ApJ*, 587, L117
 Cho, J. Y-K., & Polvani, L. M. 1996a, *Phys. Fluids*, 8, 1531
 ———. 1996b, *Science*, 273, 335
 Guillot, T., & Showman, A. P. 2002, *A&A*, 385, 156
 Henry, G. W., Marcy, G. W., Butler, R. P., & Vogt, S. S. 2000, *ApJ*, 529, L41
 Holton, J. R. 1992, *An Introduction to Dynamic Meteorology* (San Diego: Academic)
 Jha, S., et al. 2000, *ApJ*, 540, L45
 Mazeh, T., et al. 2000, *ApJ*, 532, L55
 Pedlosky, J. 1987, *Geophysical Fluid Dynamics* (2d ed.; New York: Springer)
 Rhines, P. B. 1975, *J. Fluid Mech.*, 69, 417
 Seager, S., & Sasselov, D. D. 1998, *ApJ*, 502, L157
 ———. 2000, *ApJ*, 537, 916
 Seager, S., Whitney, B. A., & Sasselov, D. D. 2000, *ApJ*, 540, 504
 Showman, A. P., & Guillot, T. 2002, *A&A*, 385, 166
 Sudarsky, D., Burrows, A., & Pinto, P. 2000, *ApJ*, 538, 885